12th International Conference on Fracture Mechanics of Concrete and Concrete Structures
FraMCoS-12
B.L.A. Pichler, Ch. Hellmich, P. Preinstorfer (Eds)

https://doi.org/10.21012/FC12.1202
MS11:4

GAS TRANSPORT BEHAVIORS OF CONCRETE DESIGNED FOR SHIELDING NUCLEAR STRUCTURES

MARTA CHOINSKA COLOMBEL[1], DARIA JÓŹWIAK-NIEDŹWIEDZKA[2] AND WOJCIECH KUBISSA[3]

[1]Nantes Université, École Centrale Nantes, CNRS, GeM, UMR 6183, F-44600 Saint-Nazaire, France, e-mail: marta.choinska@univ-nantes.fr

[2] Institute of Fundamental Technological Research, Polish Academy of Sciences, Pawińskiego 5B, 02-106 Warsaw, Poland, e-mail: djozwiak@ippt.pan.pl

[3] Faculty of Civil Engineering, Mechanics and Petrochemistry, Warsaw University of Technology, Łukasiewicza 17, 09-400 Płock, Poland, e-mail: wojciech.kubissa@pw.edu.pl

Key words: Shielding Concrete, Gas Permeability, Microstructure, Interfacial Transition Zone, Cracking

Abstract: This paper investigates the gas transport behaviors of a special type of concrete—shielding concrete—designed for use in nuclear structures, where mitigating radiation and ensuring long-term durability in harsh environments are critical.

Cracking is identified as a key factor influencing gas transport in nuclear environments, where it plays a critical role in determining material performance. In the current phase of the research, cracks and gaps, caused by significant variations in the interfacial transition zone (ITZ) and influenced by thermal treatment of concrete, depending on the type of aggregate and cement, were analyzed. Three types of concrete mixtures incorporating magnetite, serpentinite, and a combination of both aggregates are studied, alongside two types of cement: CEM I and CEM III. The transport properties of these concrete mixes, crucial for assessing their performance in nuclear shielding applications, were evaluated using three complementary methods: the Cembureau method for gas permeability, the Torrent method for measuring surface permeability, and the Air Permeability Index (API) using the Autoclam method. Additionally, microstructural analysis was conducted using scanning electron microscopy (SEM) to gain deeper insights into the material's behavior.

The impact of microcracks on permeability was examined, as such cracks often behave differently under gas transport conditions. In the next phase of the research, supplementary cracking will be intentionally induced, both mechanically and thermally, to simulate the conditions expected in typical nuclear operations.

1 INTRODUCTION

Shielding concrete is a fundamental material in nuclear power plants, medical facilities, and other environments exposed to high levels of radiation. Its dual role in containing hazardous materials and preventing radiation leakage is critical for operational safety. The primary criteria for designing concrete for shielding structures include protection against ionizing radiation as well as mechanical, physical, and durability properties under specific environmental conditions, with a particular focus on gas tightness.

The selection of concrete components considers both its durability under operational conditions and its shielding properties against

gamma and neutron radiation. Additionally, concrete must maintain low permeability throughout the facility's operational lifespan to prevent the leakage of harmful liquids and gases [1–3], thereby protecting the external environment. However, despite its dense and durable design, shielding concrete is susceptible to cracking caused by mechanical stresses, thermal cycling, and prolonged radiation exposure. These cracks can increase gas permeability, compromising the concrete's ability to contain radioactive gases and other hazardous substances while reducing its effectiveness in shielding against gamma rays and neutron radiation [1,4–6].

Concrete cracking is a complex phenomenon influenced by material composition, environmental factors, and operational conditions. Microcracks, often resulting from restrained shrinkage, due to hydration reactions or temperature gradients, gradually affect the microstructure, allowing the ingress of gases. Macrocracks, which result from microcracks coalescence, due to structural loading or external impacts, create large, interconnected pathways, significantly accelerating gas transport [7,8]. Cracks pose challenges in nuclear environments, where the release of even trace amounts of radioactive gases can have severe consequences [9]. Furthermore, cracking not only increases permeability but also disrupts the continuous dense structure required for effective radiation attenuation, leading to potential breaches in safety standards [10]. In-situ studies on concrete gas permeability used in second-generation reactors have shown that some concrete structures are nearing the allowable leakage threshold [10,11], highlighting the need for precise testing methods to quickly and accurately determine the tightness of these structures.

This study represents the first phase of a larger research initiative aimed at optimizing shielding concrete by controlling and mitigating crack propagation. The broader goal of the project is to enhance gas permeability resistance and radiation shielding effectiveness under operational conditions. In this initial phase, we investigated the gas transport behaviour of shielding concretes made with magnetite and serpentine aggregates, also with Portland cement and slag cement. The focus is on understanding how differences in aggregate type and ITZ microstructure influence discontinuities in the ITZ, crack formation and propagation. The effects of discontinuities in the ITZ on gas permeability are characterized using Cembureau permeability method, Torrent method and Autoclam method (API) test complemented by microstructural analysis through scanning electron microscopy with energy-dispersive spectroscopy (SEM-EDS).

The second phase of this project will build on these findings, implementing strategies to control crack propagation and maintain or improve the material's shielding performance. By addressing both permeability and radiation shielding in tandem, the research seeks to provide a comprehensive framework for the design of durable shielding concrete tailored to the demanding conditions of nuclear and other high-radiation applications. The insights gained from this study aim to advance international standards for concrete durability and safety in critical infrastructures.

2 MATERIALS AND METHODS

Two types of coarse aggregates: magnetite aggregates (density of 4800 kg/m³) fractions 0-5 mm and 0-16 mm and serpentine aggregates (density of 2600 kg/m³) fractions 0-2 mm, 2-8 mm and 8-16 mm were selected for their gamma and neutron shielding properties. Ordinary Portland cement CEM I 42.5 N, slag cement CEM III/A 42.5 N and siliceous sand as fine aggregate were used. Concrete mixtures were prepared with a consistent water-to-cement ratio (w/c=0.48) and adjusted superplasticizer dosages (WRA) to achieve target workability (S3 slump class), Table 1.

Table 1: Composition of the concrete mix in kg/m³

	M-I	S-I	MS-I	M-III	S-III	MS-III
cement	CEM I			CEM III		
	350	350	350	350	350	350
water	168	168	168	168	168	168
sand 0/2	371	371	371	371	371	371
mag 0/5	839	0	895	839	0	895
mag. 0/16	1846	0	0	1846	0	0
serp. 0/2	0	273	0	0	273	0
serp. 2/8	0	909	485	0	909	485

	M-I	S-I	MS-I	M-III	S-III	MS-III
cement	CEM I			CEM III		
	350	350	350	350	350	350
water	168	168	168	168	168	168
serp. 8/16	0	273	485	0	273	485
WRA	0.64	3	1.97	0.57	1.71	1.24

Three types of gas permeability test were applied: Cembureau method, Torrent method and Autoclam method. Cembureau method evaluates gas permeability by measuring nitrogen flow through a specimen at different pressures, applying Klinkenberg regression to determine the final intrinsic value. Torrent method assesses permeability by recording the pressure equalization rate after vacuum pressure (30–50 hPa) is released, calculating the kT coefficient. API method measures air permeability by monitoring pressure decay at 500 mbar over 15 minutes, with results expressed as the slope of the logarithmic pressure-time graph. Before conducting measurements using all methods, the specimens were dried to constant mass at 80°C to simulate operational and quite harsh conditions, however without inducing intuitionally any localised artificial macrocracks. Then they were conditioned for 48 hours at a temperature of 20±1°C in a desiccator. Drying at a higher temperature (105°C), as recommended in the API and Cembureau methods, was omitted due to its much severe potential impact on the microstructure of the concrete [12,13]. Due to prior research experience, cubic specimens with an edge length of 150 mm were prepared to determine compressive strength and gas permeability using the Torrent and API methods. For the Cembureau method, cylinders with a diameter of 100 mm were used instead of 150 mm diameter specimens. Smaller specimens required shorter drying times to achieve a constant mass, and this dimension was also chosen to align with further research regarding shielding properties. The Torrent test was conducted on three cubic samples, with the result reported as the average kT value from four measurements on each sample. The gas permeability results from the Cembureau method represent the average of three cylindrical sample measurements. The API test was performed on three cubic samples for each concrete series.

After conducting gas permeability tests on the cylindrical specimens, the evaluation of the concrete microstructure was performed on thin sections using optical microscope with transmitted light and plane sections using SEM-EDS. Previously cut concrete specimens (40 × 50 mm) were vacuum-impregnated with low-viscosity resin containing a yellow fluorescent dye. The sections were ground and polished using silicon carbide papers (up to 1,200 grit) and diamond paste (6, 3, 1, and 0.25 μm) to achieve a 20 ± 2 μm thickness with a mirror finish. They were analysed using an Olympus BX51 polarizing microscope with a digital camera. The preparation process of polished sections included cutting the specimens into dimensions of 25x40x10 mm, drying them for three days at 50°C, and impregnating them with epoxy resin. The samples were ground and polished. After further drying, a carbon coating (20 nm) was applied. The analysis was performed using a JEOL JSM-6460LV scanning electron microscope equipped with an EDS detector, allowing for qualitative and quantitative elemental analysis at an accelerating voltage of 20 kV, a 110 μm aperture, and a working distance of 8–9 mm. For each concrete type, at least five polished sections were analysed to determine the width of the discontinuity zone between the aggregate grains and the cement matrix.

3 RESULTS

Table 2 presents the slump, density, and compressive strength of concrete after 28 days, while Table 3 shows gas permeability results obtained using three methods. All concretes, with both Portland cement (CEM I) and slag cement (CEM III), achieved the intended S3 plastic consistency without exceeding the maximum admixture dose. Magnetite aggregate concretes exhibited the highest density (3583 kg/m³ for CEM I and 3499 kg/m³ for CEM III) and compressive strength (70 MPa for CEM I and 73 MPa for CEM III), while serpentinite aggregate concretes had lower density (2319 kg/m³) and reduced strength, with decreases of 17% for CEM I and 15% for CEM III compared to magnetite.

Table 2: The consistency test of the concrete mix, as well as the density and compressive strength of concrete after 28 days of curing.

Properties	M-I	S-I	MS-I	M-III	S-III	MS-III
Slump mm	120	90	150	130	140	140
Denisty kg/m^3	3538	2329	2723	3499	2309	2712
f_{c28} MPa	70	58	67	73	62	69

Concretes made with slag cement (CEM III) exhibited lower gas permeability compared to those made with Portland cement (CEM I), regardless of the testing method used. Among all concretes, those with serpentinite aggregate showed the highest air and nitrogen permeability, while those with magnetite aggregate had the lowest, for both types of cement. Serpentinite aggregate concretes demonstrated approximately 1.3 times (API) and almost 2 times (Cembureau) higher gas permeability compared to magnetite aggregate concretes. Air permeability measured by the Torrent method was 3 times and more than 20 times higher for serpentinite aggregate concretes compared to magnetite aggregate concretes, for CEM I and CEM III, respectively.

Table 3: Gas permeability results.

		M-I	S-I	MS-I	M-III	S-III	MS-III
Cembureau, x10^{-17} m^2	mean	1.48	2.58	2.20	0.95	2.10	1.80
	SD	0.27	0.36	0.30	0.26	0.32	0.31
kT, x10^{-16} m^2	mean	0.644	2.154	1.418	0.094	0.897	0.752
	SD	0.018	0.076	0.072	0.011	0.071	0.025
Autoclam (API) [ln(mbar)/min]	mean	0.121	0.160	0.135	0.108	0.133	0.125
	SD	0.011	0.009	0.015	0.010	0.007	0.008

SD – Standard Deviation

Thin section and SEM analysis of shielding concrete provided detailed insights into the microstructure of the cement matrix and the aggregate-matrix interfacial transition zone, Figs. 1-4. All concretes showed evenly distributed coarse and fine aggregate grains, with a uniform and dense sand grain-matrix contact layer (Fig. 1), regardless of the cement or coarse aggregate type. While concretes with magnetite aggregate displayed a compact ITZ, serpentinite aggregate concretes exhibited numerous discontinuities and voids, with defects in the serpentinite grains observed regardless of the cement type (Fig. 2).

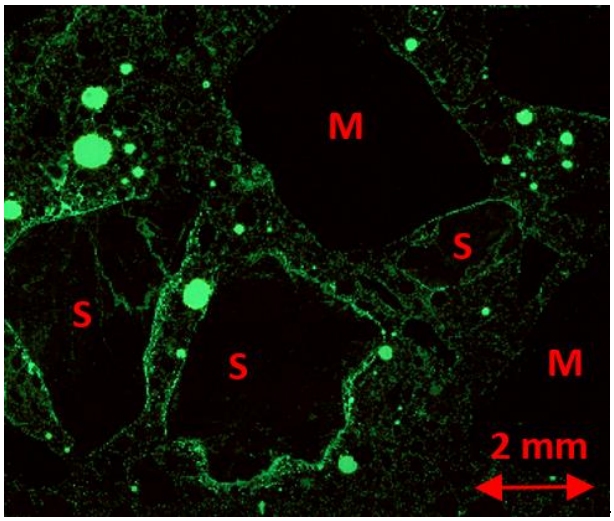

Figure 1: Microstructure of the shielding concrete with magnetite (M) and serpentinite (S) aggregate on thin section in UV light.

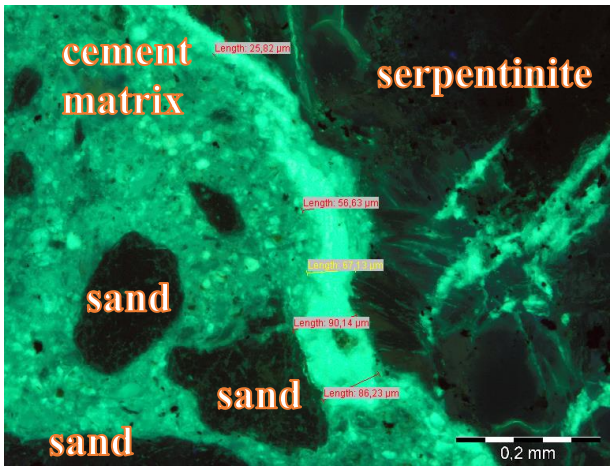

Figure 2: Microstructure of the shielding concrete with serpentinite aggregate on thin section in UV light.

SEM analysis confirmed the presence of a dense contact zone between the magnetite aggregate grains and the cement matrix (Fig. 3a) and the occurrence of discontinuity zones between the serpentinite aggregate grains and the cement paste (Figs. 3b and 4). The width of the discontinuity zone between the serpentinite aggregate grains and the cement matrix was 38.1±10.2 µm for concrete with ordinary Portland cement and 29.5±6.1 µm for slag

cement.

(a)

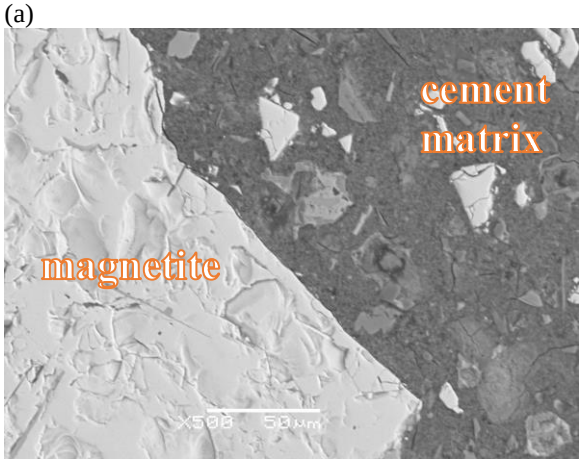

(b)

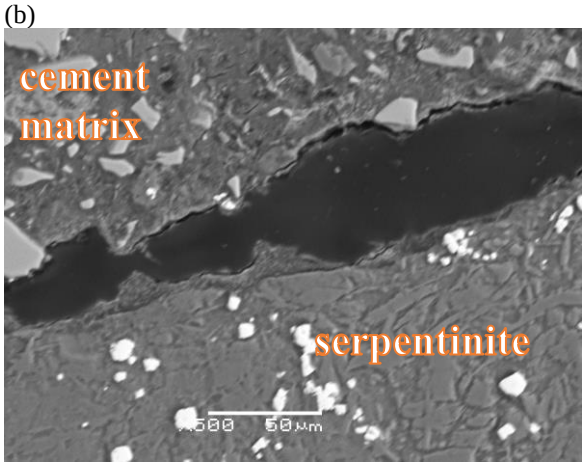

Figure 3: SEM microstructure of the shielding concrete: a) magnetite aggregate, b) serpentine aggregate; magnification x500

(a)

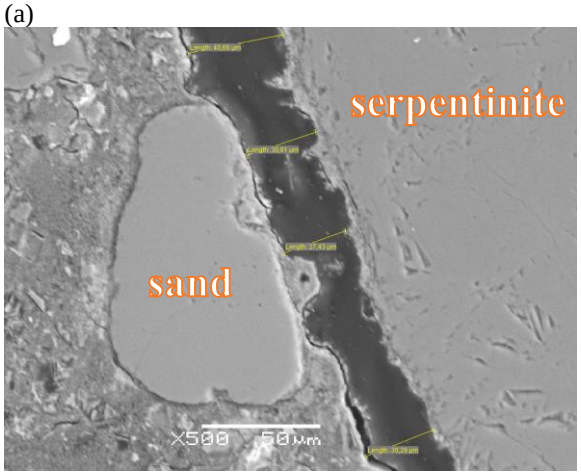

(b)

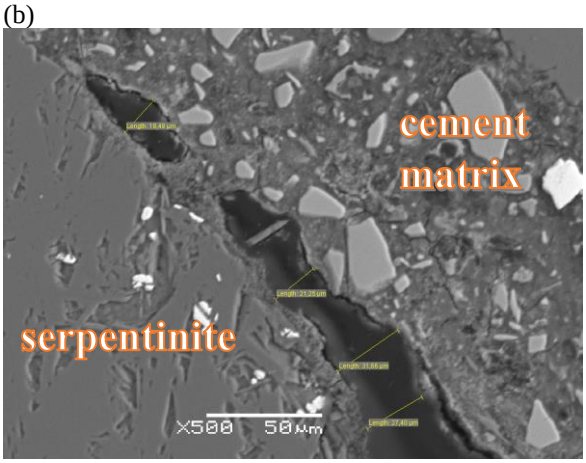

Figure 4: SEM microstructure of the shielding concrete with serpentinite aggregate: a) CEM I, S_1, b) CEM III, S_3; magnification x200

4 DISCUSSIONS

Obtained strength and permeability data as well results of the microscopic observations on thin sections of concrete and discontinuity observations are consistent with each other.

Magnetite aggregate concrete had the highest density (~3500 kg/m³), while serpentinite aggregate concrete had the lowest (~2300 kg/m³), with slightly higher densities for Portland cement (CEM I) than slag cement (CEM III). Similar density values for magnetite and serpentinite concretes were found by other researchers [14–16].

The use of serpentinite aggregate resulted in about 16% reduction in compressive strength compared to magnetite aggregate. Similar strength values were reported by Kubissa et al. [17] and Dąbrowski et al. [18], while Jain et al. [19] confirmed that serpentinite lowers concrete strength. Sayyadi et al. [20] attributed this reduction to poor hydration and weak adhesion between the paste and serpentinite aggregate, particularly with over 25% serpentinite content. Dąbrowski et al. [18] observed increased porosity in the ITZ, and Abdullah et al. [21] linked this to serpentinite's high water absorption, which leads to a more porous ITZ.

The conceptualization of ITZ discontinuities as microcracks offers a useful framework for predicting and controlling concrete's durability and performance [22, 23]. The ITZ is inherently more porous than the bulk cement matrix due to

localized effects during hydration, including water segregation and incomplete packing of cement particles [24]. This porosity creates a discontinuity between the aggregate and the matrix, which can be considered as a network of microcracks, additionally influenced by thermal treatment of concrete. In conducted tests in the serpentinite aggregate concretes, the ITZ exhibited larger discontinuities (up to 38.1 ± 10.2 μm) compared to magnetite aggregate concretes, which had a denser ITZ structure. These microcracks serve as pathways for gas movement, contributing to higher permeability. The type of aggregate significantly affects the ITZ [25]. Magnetite aggregates, characterized by their high density and low water absorption, promote a tightly packed ITZ with strong adhesion to the cement matrix. This results in lower permeability values, as confirmed by all testing methods in the study. Conversely, serpentinite aggregates, with higher water absorption and weaker bonding properties, lead to a more porous ITZ. The increased microcracking in serpentinite concretes directly correlates with higher gas permeability, as observed for example in the Torrent method results, which showed permeability values up to 2.154×10^{-16} m², more than twenty times higher than magnetite concretes with slag cement.

Cracking significantly impacts gas transport, with microcracks dominating permeability in serpentinite concretes and macrocracks expected to play a more critical role under operational conditions. Microcracks primarily impact serpentinite concretes due to their expansive ITZ. However, macrocracks, though not induced, are anticipated to dominate permeability in real-world nuclear operations, requiring further studies under simulated operational loads.

Future studies will focus on modifying the ITZ microstructure through advanced admixtures or alternative cementitious materials to enhance bonding and reduce porosity. Simultaneously, understanding the mechanisms of microcrack coalescence into macrocracks under operational loads is crucial for long-term durability assessments of critical infrastructure materials.

In nuclear environments, where gas containment is critical, the permeability of concrete directly impacts its ability to confine radioactive gases. The findings of this study emphasize the importance of ITZ quality in achieving low permeability. Magnetite aggregates combined with slag cement represent the optimal solution for minimizing gas permeability. However, further innovation is required to enhance the performance of serpentinite concretes, which offer superior neutron shielding but are hindered by their high ITZ porosity.

5 CONCLUSIONS

This study confirms the key role of material selection and therefore microstructure and especially the aggregate-cement matrix contact zone in determining the gas transport behaviour of protective concretes.

Based on the conducted research, the following conclusions can be drawn:

- Permeability measurements using Cembureau, Torrent, and Autoclam methods confirmed the superior performance of magnetite concretes in minimizing gas transport.
- Concretes made with slag cement (CEM III) demonstrated lower gas permeability across all testing methods compared to those with Portland cement (CEM I)
- Magnetite aggregates and slag cement (CEM III) demonstrated superior impermeability, while serpentinite concretes exhibited higher gas permeability due to ITZ porosity and microcracking.
- ITZ microcracks, particularly in serpentinite concretes, pose risks for nuclear shielding structures by enabling gas transport under stress or thermal cycling. On the one hand, there is a critical need for methods to reduce ITZ microcracking. On the other hand, understanding the behavior of shielding concrete under severe nuclear conditions remains a key research priority.

REFERENCES

[1] M.A. Glinicki, Long-Term Performance of Concrete in Shielding Structures of

Nuclear Power Plants, IPPT PAN, Warsaw, 2015.

[2] G. Nahas, J.M. Torrenti, Durability and safety of concrete structures in the nuclear context, in: Concrete Under Severe Conditions, Two Volume Set, CRC Press, 2010: pp. 31–46. https://doi.org/10.1201/b11817-2.

[3] I. Remec, K.G. Field, D.J. Naus, T.M. Rosseel, J.T. Busby, Concrete aging and degradation in NPPs: LWRS program R\&D progress report, Trans Am Nucl Soc 109 (2013) 403–406.

[4] K.G. Field, I. Remec, Y. Le Pape, Radiation effects in concrete for nuclear power plants – Part I: Quantification of radiation exposure and radiation effects, Nuclear Engineering and Design 282 (2015) 126–143. https://doi.org/10.1016/j.nucengdes.2014.10.003.

[5] P.A. Rasheed, S.K. Nayar, I. Barsoum, A. Alfantazi, Degradation of Concrete Structures in Nuclear Power Plants: A Review of the Major Causes and Possible Preventive Measures, Energies (Basel) 15 (2022) 8011. https://doi.org/10.3390/en15218011.

[6] H.Ş. Arel, E. Aydin, S.D. Kore, Ageing management and life extension of concrete in nuclear power plants, Powder Technol 321 (2017) 390–408. https://doi.org/10.1016/j.powtec.2017.08.053.

[7] R. Torrent, G. Frenzer, A method for the rapid determination of the coefficient of permeability of the ‘“covercrete’’’",”’ in: W.G. Schickert, H. Wiggenhauser (Eds.), International Symposium Non-Destructive Testing in Civil Engineering (NDT-CE), 1995: pp. 985–992.

[8] M.H. Nguyen, K. Nakarai, Y. Kai, S. Nishio, Early evaluation of cover concrete quality utilizing water intentional spray tests, Constr Build Mater 231 (2020) 117144. https://doi.org/10.1016/j.conbuildmat.2019.117144.

[9] Ageing management of concrete structures in nuclear power plants, IAEA Nuclear Energy Series No. NP-T-3.5 (2016) 372.

[10] Y. Pei, S. Li, F. Agostini, F. Skoczylas, B. Masson, Sealing of concrete confining structures of French nuclear reactors, Eng Struct 197 (2019). https://doi.org/10.1016/j.engstruct.2019.109283.

[11] F. Agostini, F. Skoczylas, B. Masson, Sealing of concrete confining structures of French nuclear reactors, in: A.M. Brandt, J. Olek, M.A. Glinicki, Ch.K.Y. Leung, J. Lis (Eds.), 11th International Symposium on Brittle Matrix Composites BMC 2015, IPPT PAN, Warszawa, 2015: pp. 343–352.

[12] Q.B. Travis, B. Mobasher, Correlation of Elastic Modulus and Permeability in Concrete Subjected to Elevated Temperatures, Journal of Materials in Civil Engineering 22 (2010) 735–740. https://doi.org/10.1061/(ASCE)MT.1943-5533.0000074.

[13] M. Choinska, A. Khelidj, G. Chatzigeorgiou, G. Pijaudier-Cabot, Effects and interactions of temperature and stress-level related damage on permeability of concrete, Cem Concr Res 37 (2007) 79–88. https://doi.org/10.1016/j.cemconres.2006.09.015.

[14] P. Lehner, J. Gołaszewski, Relationship of Different Properties from Non-Destructive Testing of Heavy Concrete from Magnetite and Serpentinite, Materials 14 (2021) 4288. https://doi.org/10.3390/ma14154288.

[15] A.S. Ouda, Development of high-performance heavy density concrete using different aggregates for gamma-ray shielding, Progress in Nuclear Energy 79 (2015) 48–55. https://doi.org/10.1016/j.pnucene.2014.11.009.

[16] E. Horszczaruk, P. Brzozowski, Investigation of gamma ray shielding efficiency and physicomechanical performances of heavyweight concrete subjected to high temperature, Constr Build Mater 195 (2019) 574–582. https://doi.org/10.1016/j.conbuildmat.2018.09.113.

[17] W. Kubissa, M.A. Glinicki, M. Dąbrowski, Permeability testing of radiation shielding concrete manufactured at industrial scale, Mater Struct 51 (2018) 83. https://doi.org/10.1617/s11527-018-1213-0.

[18] M. Dąbrowski, D. Jóźwiak-Niedźwiedzka, K. Bogusz, M.A. Glinicki, Influence of serpentinite aggregate on the microstructure and durability of radiation shielding concrete, Constr Build Mater 337 (2022) 127536. https://doi.org/10.1016/j.conbuildmat.2022.127536.

[19] A. Jain, V. Agrawal, R. Gupta, Using serpentine in concrete: A literature review, Mater Today Proc (2023). https://doi.org/10.1016/j.matpr.2023.03.138.

[20] A. Sayyadi, Y. Mohammadi, M.R. Adlparvar, Effect of Serpentine Aggregates on the Shielding, Mechanical, and Durability Properties of Heavyweight Concrete, International Journal of Engineering 35 (2022) 2256–2264. https://doi.org/10.5829/IJE.2022.35.11B.21.

[21] M.A.H. Abdullah, R.S.M. Rashid, M. Amran, F. Hejazii, N.M. Azreen, R. Fediuk, Y.L. Voo, N.I. Vatin, M.I. Idris, Recent Trends in Advanced Radiation Shielding Concrete for Construction of Facilities: Materials and Properties, Polymers (Basel) 14 (2022) 2830. https://doi.org/10.3390/polym14142830.

[22] C.E. Torrence, J.E. Trageser, R.E. Jones, J.M. Rimsza, Sensitivity of the strength and toughness of concrete to the properties of the interfacial transition zone, Constr Build Mater 336 (2022) 126875. https://doi.org/10.1016/j.conbuildmat.2022.126875.

[23] G. Ramesh, E. D. Sotelino, and W.-F. Chen, “Effect of Transition Zone on Elastic Stresses in Concrete Materials,” J. Mater. Civil Eng., 10[4] 275–82 (1998).

[24] J. P. Ollivier, J. C. Maso, and B. Bourdette, “Interfacial Transition Zone in Concrete,” Adv. Cem. Based Mater., 2[1] 30–8 (1995)

[25] T. Akçaoğlu, M. Tokyay, T. Çelik, Effect of coarse aggregate size and matrix quality on ITZ and failure behavior of concrete under uniaxial compression, Cement and Concrete Composites, 26 (6) 2004, 633-638, https://doi.org/10.1016/S0958-9465(03)00092-1.